

Brief Report

Characterization of Biochars Produced from Dairy Manure at High Pyrolysis Temperatures

Wen-Tien Tsai ^{1,*}, Po-Cheng Huang ² and Yu-Quan Lin ²

¹ Graduate Institute of Bioresources, National Pingtung University of Science and Technology, Pingtung 912, Taiwan

² Department of Environmental Science and Engineering, National Pingtung University of Science and Technology, Pingtung 912, Taiwan; mike299123@gmail.com (P.-C.H.); wsx55222525@gmail.com (Y.-Q.L.)

* Correspondence: wtttsai@mail.npust.edu.tw; Tel.: +886-8-770-3202

Received: 20 August 2019; Accepted: 9 October 2019; Published: 14 October 2019



Abstract: In this work, the thermochemical analyses of dairy manure (DM), including the proximate analysis, ultimate (elemental) analysis, calorific value, thermogravimetric analysis (TGA), and inorganic elements, were studied to evaluate its potential for producing DM-based char (DMC) with high porosity. The results showed that the biomass should be an available precursor for producing biochar materials based on its high contents of carbon (42.63%) and volatile matter (79.55%). In order to characterize their pore properties, the DMC products produced at high pyrolysis temperatures (500–900°C) were analyzed using surface area and porosity analyzer, pycnometer, and scanning electron microscopy-energy dispersive X-ray spectroscopy (SEM-EDS). The values of pore properties for the DMC products increased with an increase in pyrolysis temperature, leading to more pore development and condensed aromatic cluster at elevated temperatures. Because of the microporous and mesoporous structures from the N₂ adsorption–desorption isotherms with the hysteresis loops (H4 type), the Brunauer–Emmett–Teller (BET) surface area of the optimal biochar (DMC-900) was about 360 m²/g, which was higher than the data reported in the literature. The highly porous structure was also seen from the SEM observations. More significantly, the cation exchange capacity (CEC) of the optimal DMC product showed a high value of 57.5 ± 16.1 cmol/kg. Based on the excellent pore and chemical properties, the DMC product could be used as an effective amendment and/or adsorbent for the removal of pollutants from the soil media and/or fluid streams.

Keywords: dairy manure; thermochemical property; pyrolysis; biochar; pore property

1. Introduction

Since the Kyoto Protocol adopted on 11 December 1997, humans are beginning to actively focus on mitigating greenhouse gas (GHG) emissions because it is irreversibly changing the planet's ecosystems via global warming. In this regard, the livestock sector plays a significant role in the globally anthropogenic emissions of GHG, including carbon dioxide (CO₂), methane (CH₄), and nitrous oxide (N₂O) [1]. According to the statistical data by the Food and Agriculture Organization [2], cattle-raising and its resulting manure are the most important contributors to the sector's GHG emissions, accounting for 65% of the livestock sector emissions. Regarding the main sources of emissions from the sector, the deposition of cattle manure on pastures and manure storage and processing generate substantial amounts of GHG. In order to mitigate GHG emissions and upgrade the recycling of nutrients and lignocellulosic sources, the thermochemical processes (e.g., pyrolysis) can convert cattle manure into renewable chemicals like char or biochar [3]. More importantly, this manure treatment can gain several positive benefits, including GHG emission reduction, biomass nutrients recycling, biofuels and carbon materials production, and waste management without public health concerns [4].

Among the thermochemical processes, pyrolysis is an available method to convert cattle manure into biofuels and/or chemicals. In the process, the lignocellulosic components of the biomass are broken down condensable hydrocarbon molecules (e.g., acetic acid), noncondensable gases (e.g., CO₂), and solid carbon as char or biochar under an inert atmosphere. Based on the heating rate, the pyrolysis technology may be divided into slow and fast processes [5]. The slow pyrolysis process (≤ 10 °C/min) is used primarily for the production of biochar at higher temperatures (≥ 400 °C), but the fast pyrolysis process (≥ 100 °C/min) primarily for the production of bio-oils is at about 500 °C [6–8]. Furthermore, the resulting biochar not only provides a remarkable carbon sink for mitigating GHG emissions, but also possesses available pore structure for its potential use as an adsorbent and/or soil amendment [9].

Biochar is a rigid and porous carbon material. Its pore properties, however, vary over a wide range with its precursor type and production conditions [5]. Although there are many research studies for reusing dairy (cattle) manure (DM) as a feedstock for char production, few studies focused on the production of dairy manure-based char (DMC) at higher temperatures [3,10–17]. These studies almost produced biochars at a moderate temperature (300–700 °C). It is notable that their pore properties were not significant. For instance, Cantrell et al. [3] reported the physicochemical results for five manure-based biochars pyrolyzed at 350 °C and 700 °C, showing that the specific surface area (SSA) of DMC produced at 700 °C was 186.5 m²/g. However, the SSA value of DMC produced at 700 °C in another study was only 74.0 m²/g [17]. On the other hand, the biochars obtained at higher pyrolysis temperatures showed more stability in both abiotic and biotic incubations [18].

As reviewed above, there is very limited research focused on the production of biochar at higher pyrolysis temperatures (>700 °C) in the literature [19,20]. In the previous studies [21–23], the authors even investigated the thermochemical characterization of DM with relevance to its energy conversion and environmental implications. In order to evaluate DM as a precursor for producing biochars as solid fuels, the authors further prepared DMC products at 400–800 °C [21], suggesting that its resulting chars can be used as clean solid fuels based on their high values of carbon (60% by weight, or 60 wt%) and calorific value (22.3 MJ/kg), and low contents of nitrogen (0.5 wt%). In the preliminary evaluation [23], a biochar product was produced at 900 °C, showing its microporous/mesoporous textures with a specific surface area of about 300 m²/g. In the present study, a series of DMC products, produced at higher charring temperatures (i.e., 500–900 °C), were used to see the structural changes based on their pore properties and true densities.

2. Materials and Methods

2.1. Materials

The dairy manure (DM) for producing biochar was obtained from the livestock farm at the National Pingtung University of Science and Technology (Pingtung, Taiwan). Details on the DM pretreatment were described in the previous studies [21–23].

2.2. Thermochemical Analysis of Oven-Dried DM

In this work, the thermochemical properties of DM, including proximate analysis, ultimate (elemental) analysis, calorific (heating) value, inorganic elements, and thermogravimetric analysis (TGA), were conducted to evaluate the potential for producing porous biochar at adequate pyrolysis conditions. Again, details on the thermochemical analysis of oven-dried DM were described previously [21–23].

2.3. Pyrolysis Experiments

Because the temperature has been shown to be the most important process parameter in the pyrolysis experiments [11,24], the DMC products were produced at higher pyrolysis temperatures (500–900 °C), moderate residence time (30 min), and low heating rate (10 °C/min) under an inert atmosphere by nitrogen flow. The pyrolysis conditions were similar to the previous study [21], except

for the pyrolysis temperature. The yields of the DMC products were obtained by the difference between the weights of DM (5 g for each experiment) and DMC. The DMC products produced at 500, 600, 700, 800, and 900 °C were marked as DMC-500, DMC-600, DMC-700, DMC-800, and DMC-900, respectively.

2.4. Characterization of DMC

As mentioned above, the main purpose was to produce biochars with high pore properties (including specific surface area, pore volume, and porosity). Therefore, the physical characterization of DMC was mainly based on the nitrogen adsorption–desorption isotherms and true density by using a surface area and porosity analyzer (Model No.: ASAP 2020; Micromeritics Co., Norcross, GA, USA) and a gas pycnometer (Model No.: AccuPyc 1340; Micromeritics Co., Norcross, GA, USA), respectively. More details about the analytical conditions were determined previously [25,26]. On the other hand, the microstructural textures and elemental compositions on the surface of DM and DMC were measured by using a scanning electron microscopy (Model No.: S-3000N; Hitachi Co., Tokyo, Japan) coupled with an energy dispersive X-ray spectroscopy (Swift ED3000, Oxford Instruments, Abingdon, UK). Regarding the chemical characterization of DMC, it included proximate analysis, ultimate (elemental) analysis, and calorific value, which were similar to the thermochemical analysis of oven-dried DM in the Section 2.2.

3. Results and Discussion

3.1. Thermochemical Characterization of Dairy Manure (DM)

As shown in Table 1, there were high contents of carbon (C, 42.63%) and hydrogen (H, 6.43%) in the dried dairy manure (DM), which was consistent with the high value of volatile matter (79.55%) due to the undigested lignocellulose. The compositional characterization should be attributed to ruminant feed (or forage) like pangola grass and napier grass. Making a comparison between the molar ratios of DM ($C_6H_{10.9}$) and cellulose ($C_6H_{10}O_5$)/hemicellulose ($C_5H_8O_4$), their values were approximate to each other. Therefore, its calorific value was up to 18.4 MJ/kg-dry. The data in Table 1 were very close to those in the previous studies [25,26] and other reports [27–29]. On the other hand, the contents of inorganic elements in the biochar precursor (i.e., DM) will be important for various reasons, including soil fertility and contamination when reusing it (or resulting biochar) as an organic fertilizer, and slagging and fouling as it was burned in boilers. In this regard, the macro-nutrients (i.e., Ca, Mg, P, Si, K), micro-nutrients (i.e., Mn, Cu, Zn, Fe), and toxic metals (i.e., As, P, Cd, Cr) in the DM were determined in the present study based on the analyses of inductively coupled plasma-optical emission spectrometer (ICP-OES). These inorganic elements in the DM biomass will exist in the so-called ash, which is as high as 10.94% (Table 1). Also, the oxides or carbonates of alkali metals (i.e., K, Na) and alkaline earth metals (i.e., Ca, Mg, Sr, Ba) from the DM ash could evaporate at combustion temperature due to the relatively low melting points and subsequently condense on the down streams. As listed in Table 2, the primary inorganic elements included calcium (Ca), silicon (Si), phosphorus (P), magnesium (Mg), potassium (K), sodium (Na), and aluminum (Al). The contents of these ash-forming elements in DM were in accordance with those in grass biomass such as straw [30]. These inorganic elements could be present in the forms of oxide or carbonate like SiO_2 , CaO, or $CaCO_3$. Regarding the concentrations of toxic metals in DM, the ash is almost free of them, including arsenic (As), cadmium (Cd), chromium (Cr), cobalt (Co), copper (Cu), nickel (Ni), and lead (Pb). However, it should be noted that the contents of zinc (Zn) and manganese (Mn) in Table 2 indicated small amounts (0.017% and 0.034%, respectively). Although these contents were significantly lower than the swine-based manure [31], their moderate toxicity may pose hazards to ecosystems.

Table 1. Proximate analysis, ultimate analysis, and calorific value of dairy manure (DM).

Property	Value ^a
Proximate analysis (wt%) ^a	
Volatile matter	79.55 ± 0.19
Ash content	10.94 ± 0.27
Fixed carbon ^b	9.51
Ultimate analysis (wt%) ^a	
Carbon (C)	42.63 ± 0.01
Hydrogen (H)	6.43 ± 0.08
Oxygen (O)	39.70 ± 0.03
Nitrogen (N)	2.01 ± 0.13
Sulfur (S)	0.42 ± 0.02
Calorific value (MJ/kg) ^a	18.40 ± 0.08

^a On a dry basis; two or three measurements. ^b By difference.

Table 2. Contents of relevant trace elements of dairy manure (DM).

Inorganic Element	Value ^a	Method Detection Limit (ppm)
Ca (wt%)	2.140	8.4
Si (wt%)	1.130	11.3
P (wt%)	0.822	91.8
Mg (wt%)	0.642	5.4
K (wt%)	0.426	51.6
Na (wt%)	0.202	11.4
Al (wt%)	0.107	17.4
Fe (wt%)	0.081	6.6
Mn (wt%)	0.034	6.0
Zn (wt%)	0.017	4.2
Sr (wt%)	0.007	0.3
Ti (wt%)	0.006	1.2
Ba (wt%)	0.002	0.3
As (wt%)	ND ^b	0.5
Cd (wt%)	ND	2.4
Cr (wt%)	ND	7.8
Co (wt%)	ND	20.4
Cu (wt%)	ND	7.2
Ni (wt%)	ND	19.2
Pb (wt%)	ND	17.4

^a On a dry basis (moisture free). ^b Not detectable.

In the measurement of thermogravimetric analysis (TGA), the TGA curve of DM (0.2 g), shown in Figure 1, was obtained at a heating rate of 10 °C/min under the nitrogen flow (50 cm³/min). Obviously, there were three stages for the devolatilization and carbonization of biomass (i.e., DM) biopolymer constituents (i.e., hemicellulose, cellulose, and lignin) in different temperatures [5]. The first stage in the temperature range of 25–200 °C represented the thermal desorption of moisture attached and structural deformity of the biomass. The second stage ranging from 250 to 450 °C was the greatest change on the mass lose zone. From the derivative thermogravimetric (DTG) curve, the pyrolytic decompositions of hemicellulose and cellulose occurred at the peak temperatures of around 320 °C and 380 °C, respectively. This reaction zone was indicative of extensive decomposition of hemicellulose in the early stage due to its fragile structure chemically in comparison with cellulose and lignin. Subsequently, cellulose started to undergo decomposition reactions such as devolatilization and carbonization. The third stage starting from 430 °C was attributed to the rigorous decompositions of lignin and its resulting char, making it brittle and porous. In this regard, the pyrolysis temperature was adopted at above 500 °C in the charring experiments for producing porous biochars.

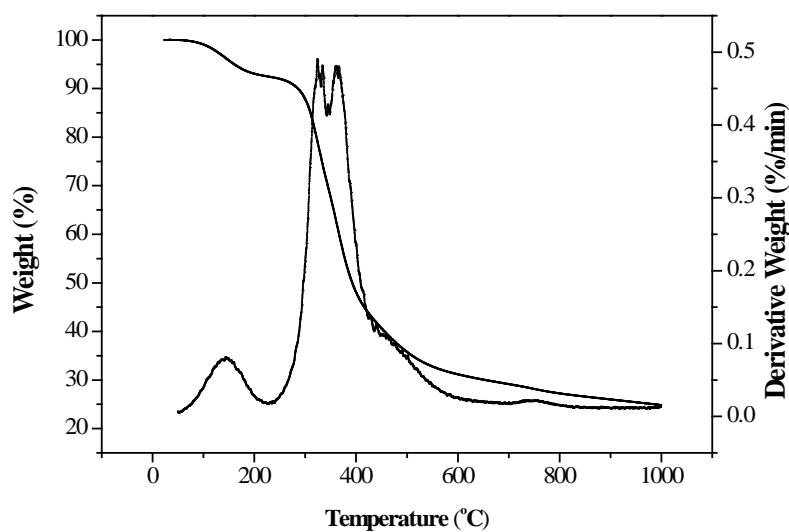


Figure 1. Thermogravimetric analysis (TGA) and derivative thermogravimetry (DTG) curves at heating rate of 10 °C/min for dairy manure (DM).

3.2. Yield and Pore Properties of DMC Products

For better utilization in the agricultural and environmental applications, the yields, densities, and pore properties of DMC products were determined in this work. As shown in Figure 2, the yields, ranging from 31.4% to 22.5%, indicated a decreasing trend as the pyrolysis temperature was increased from 500 °C to 900 °C. This variation should be attributed to the devolatilization and carbonization of solid char products during the progressive pyrolysis at higher temperatures, which was consistent with the TGA observations (Figure 1).

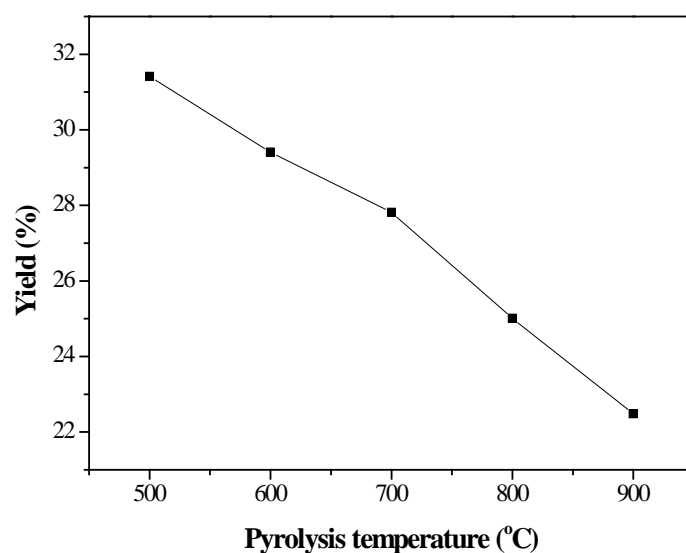


Figure 2. Yields of DM-derived biochar (DMC) as a function of pyrolysis temperature.

The pore properties of material involve the correlations between its specific surface area, pore volume, and density. Among them, specific surface area may be the most important parameter to indicate the adsorptive capacity and the quality of biochar. Based on the Brunauer–Emmett–Teller (BET) model, it was commonly measured by N₂ adsorption–desorption isotherms at −196 °C using the surface area and porosity analyzer. Table 3 summarized the pore properties of DMC products produced at various pyrolysis temperatures [32,33]. The true density is defined as the ratio of the biochar mass to the volume occupied by that mass, which was measured by a helium-displacement

pycnometer. However, the particle density was estimated by the total pore volume and true density. Based on the definition of porosity in the porous particle, this property was further determined by the particle density and the true density. The data in Table 3 obviously indicated an increasing trend in pore properties, including the BET surface area, micropore area, total pore volume, micropore volume, true density (ρ_s), particle density (ρ_p), and porosity (ϵ_p). This result was in accordance with the observations of the average pore diameter (D_{ave}), DMC's yield, and the DM's TGA, suggesting that the rigorous carbonization (charring) at higher pyrolysis temperatures was favorable to the development of porous structure in the DMC products with aromatic carbon clusters [34]. Here, assuming that the pore is of cylindrical geometry, the data on D_{ave} were calculated from the ratio of the total pore volume (V_t) and the BET surface area (S_{BET}) and can be further validated in the pore size analysis. Consistently, more condensed aromatic structure of the charring materials can be formed at higher pyrolysis temperatures (>700 °C). Therefore, the optimal DMC product (i.e., DMC-900) with the maximal BET surface area of 360.6 m²/g and true density of 2.2284 g/cm³ was produced at 900 °C. Based on the suggestion by Keiluweit et al. [35], the DMC-900 product could be a turbostratic biochar.

Table 3. Pore properties and densities of DMC products at different temperatures (500–900 °C) held for 30 min.

Biochar Product	S_{BET} ^a (m ² /g)	S_{micro} ^b (m ² /g)	V_t ^c (cm ³ /g)	V_{micro} ^d (cm ³ /g)	D_{ave} ^e (Å)	ρ_s ^f (g/cm ³)	ρ_p ^g (g/cm ³)	ϵ_p ^h (-)
DMC-500	6.5	3.3	0.008	0.002	51.2	1.6838	1.6603	0.014
DMC-600	42.9	36.3	0.030	0.020	28.2	1.8741	1.7737	0.054
DMC-700	139.1	114.3	0.088	0.063	25.2	2.0108	1.7094	0.150
DMC-800	267.6	198.5	0.167	0.109	24.9	2.1245	1.5694	0.275
DMC-900	360.6	256.7	0.240	0.141	26.6	2.2824	1.4746	0.354

^a BET surface area (S_{BET}) based on the relative pressure (P/P_0) ranging from 0.05 to 0.30. ^b Micropore area (S_{micro}) by t -plot method. ^c Total pore volume (V_t) obtained at relative pressure of about 0.95. ^d Micropore volume (V_{micro}) by t -plot method. ^e Calculated from the ratio of the total pore volume (V_t) and the BET surface area (S_{BET}) if the pore is of cylindrical geometry (i.e., average pore width = $4 \times V_t/S_{BET}$) [32,33]. ^f Measured by a pycnometer. ^g Estimated by the values of total pore volume (V_t) and true density (ρ_s) (i.e., $\rho_p = 1/[V_t + (1/\rho_s)]$) [32,33]. ^h Estimated by the values of particle density (ρ_p) and true density (ρ_s) (i.e., $\epsilon_p = 1 - \rho_p/\rho_s$) [32,33].

As mentioned above, the nitrogen (N_2) adsorption–desorption isotherms is commonly used to analyze the porous characterization of carbon material. Furthermore, the pore size distributions of the resulting biochars at the desorption branch were obtained by the Barrett–Joyner–Halenda (BJH) method [36]. Figures 3 and 4 depicted the N_2 adsorption–desorption isotherms (at -196 °C) and pore size distribution curves of DMBC products, respectively. The isotherms in Figure 3 showed type I shape, as expected for microporous materials because of its high adsorption potential at relative pressure (P/P_0) of less than 0.05. Obviously, a sharp “knee” point near P/P_0 around 0.05 was observed in these isotherms, which corresponds to the monolayer capacity. However, the specific surface area was commonly calculated from the values of P/P_0 in the range of 0.05–0.30 [36]. As shown in Figure 3, the steep increase in the isotherm slope up to P/P_0 (above 0.95) can be explained by capillary condensation within the pores, followed by saturation as the pores become filled with nitrogen liquid. The significant increase in pore properties occurred when the pyrolysis temperature was between 600 and 900 °C which should be due to the rigorous charring and shrinking reactions, thus developing more porous structures in the DMC products (i.e., DMC-700, DMC-800, and DMC-900). On the other hand, the hysteresis loop observed in the isotherms (Figure 3) is a typical Type IV for mesoporous materials. According to the classification by the International Union of Pure and Applied Chemistry (IUPAC), the DMBC products should be classified as being of the H4 type [36], indicating that the resulting biochar products are complex carbon materials containing both micropores and mesopores. More consistently, their pore size distributions observed in Figure 4 indicated two narrow profiles for micropores (<2.0 nm) and mesopores (about 4.0 nm), respectively.

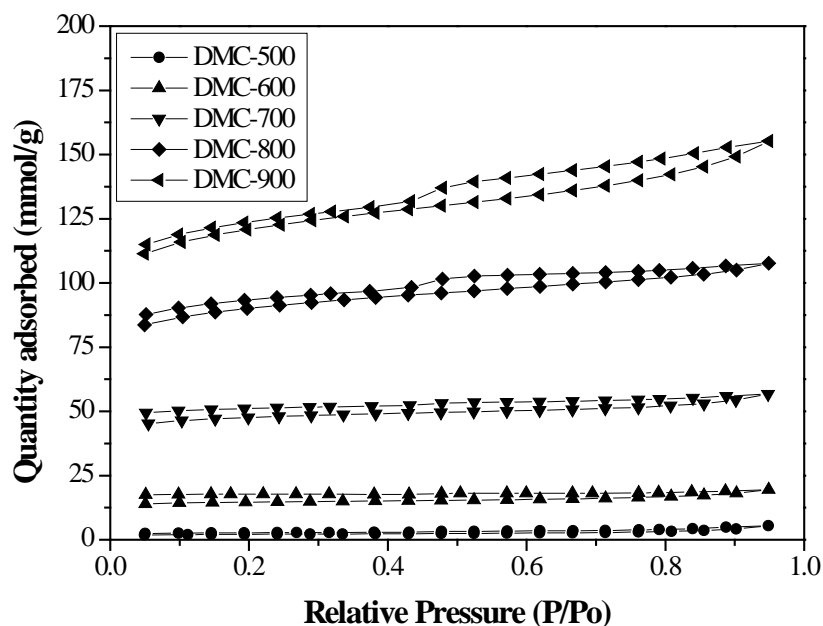


Figure 3. N_2 adsorption–desorption isotherms of DMC products (i.e., DMC-500, DMC-600, DMC-700, DMC-800, and DMC-900).

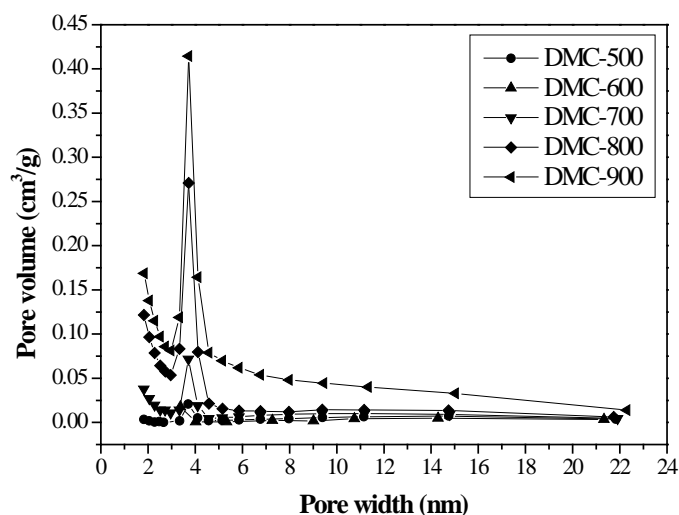


Figure 4. Pore size distributions of DMC products (i.e., DMC-500, DMC-600, DMC-700, DMC-800, and DMC-900).

In order to see the porous textures, the SEM observations were performed on the surface of DM and DMC products. Figure 5 showed the SEM micrographs ($\times 1000$) of DM and optimal DMC product (i.e., DMC-900). As seen in Figure 5a, the DM exhibited a rigid and compact matrix, which was indicative of its non-porous and rod-like features due to the lignocellulosic composition. By comparison, the optimal biochar product (DMC-900) displayed porous structures on the surface. The SEM observations were very consistent with their pore properties (Table 3). In addition, these findings were similar to the literature survey by Mukome and Parikh [37].

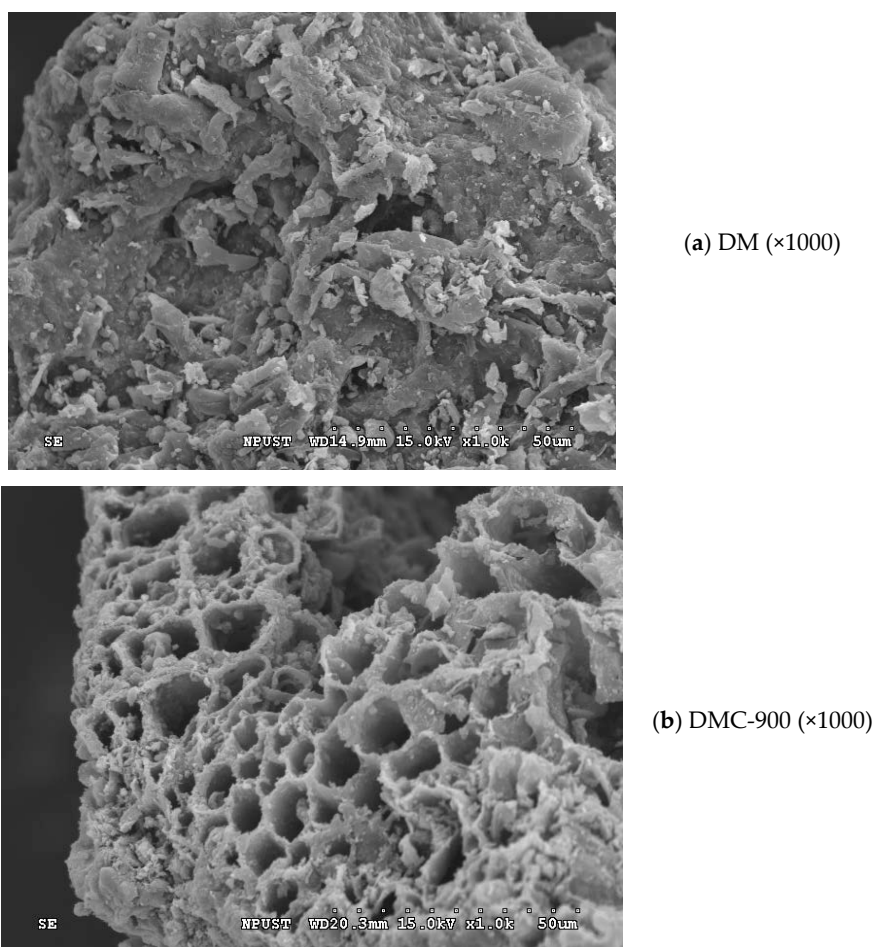


Figure 5. SEM images ($\times 1000$) of (a) dairy manure (DM), and (b) optimal biochar product (DMC-900).

3.3. Chemical Characterization of DMC Products

In order to correlate the chemical and agronomic properties of DMC products with pyrolysis temperature, Table 4 provided the data on the proximate analysis (ash content), ultimate (elemental) analysis (C/N), and calorific value. Obviously, the ash contents of DMC products indicated an upward trend, increasing from 25.26 wt% to 42.21 wt% as pyrolysis temperature increased. However, the calorific values of DMC products pyrolyzed from 500 °C to 700 °C slightly increased as their carbon contents increased, but they then decreased above 700 °C due to the decrease in the carbon content and/or the increase in the ash content. Compared to the data in Table 1, this can be further confirmed by the increase in the carbon content from 42.6 wt% to above 50 wt%, clarifying that the carbon content in the biochar products (i.e., DMC) significantly increased during the carbonization process. It should be noted that increasing the carbonization temperature from 800 °C to 900 °C will induce more gasification reaction, thus indicating a decrease in the carbon content of the resulting biochar product (Table 4). On the other hand, the nitrogen contents of the biochar products (i.e., DMC) indicated a decreasing trend. It can be ascribed to increase the emissions of N-containing pyrolytic gases at higher carbonization temperatures.

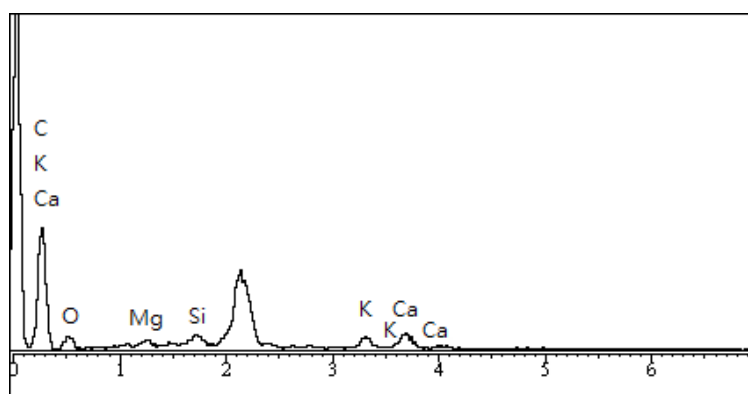
Figure 6 showed the elemental compositions on the surfaces of the optimal product DMC-900 by the energy dispersive X-ray spectroscopy (EDS). The contents of inorganic elements were consistent with the data in Table 2. It can be seen that the content of oxygen in the DMC-900 was still high, suggesting that the polar nature (i.e., hydrophilicity) enhanced by oxygen-containing functional groups on the surface will be more significant [33]. Furthermore, the cation exchange capacity (CEC) of the optimal product DMC-900 was determined in duplicate by the sodium acetate method to show a high value of 57.5 ± 16.1 cmol/kg probably due to its high specific surface area and the presence of

O-containing functional groups [37]. Therefore, the reuse of biochar as a soil amendment has been shown to increase soil CEC through electrostatic interaction due to its negatively charged surface [38]. In order to increase the biochar CEC by embedding more acidic oxygen functional groups on the surface, biochar was further treated with strong oxidants like hydrogen peroxide [39] and ozone [40]. Therefore, the removal of cationic pollutants (e.g., heavy metal ions, cationic dye) from aqueous solutions by using DM-based biochars has been widely studied in the literature [10–17].

Table 4. Chemical properties of DMC products at different temperatures (500–900 °C) held for 30 min.

Biochar Product	Proximate Analysis (wt%) ^a		Ultimate Analysis (wt%) ^a		Calorific Value ^a (MJ/kg)
	Ash	Combustible ^b	Carbon	Nitrogen	
DMC-500	25.26 ± 0.03	74.74	50.69 ± 0.75	1.99 ± 0.02	19.38 ± 0.11
DMC-600	27.56 ± 0.31	72.44	52.52 ± 0.71	1.62 ± 0.02	19.92 ± 0.10
DMC-700	29.48 ± 0.32	70.52	53.33 ± 0.71	1.43 ± 0.04	20.38 ± 1.04
DMC-800	32.65 ± 0.42	67.35	53.61 ± 0.06	1.25 ± 0.07	19.67 ± 0.03
DMC-900	42.21 ± 0.06	57.79	50.51 ± 0.09	0.78 ± 0.02	19.72 ± 0.32

^a On a dry basis; two measurements. ^b Including volatile matter and fixed carbon. It was calculated by difference.



Element	Weight %	Atomic %
Carbon	71.91	81.88
Oxygen	15.50	13.25
Calcium	5.75	1.96
Potassium	3.71	1.30
Silicon	1.91	0.93
Magnesium	1.22	0.68

Figure 6. Energy-dispersive X-ray spectrometry (EDS) analyses of optimal biochar product (i.e., DMC-900).

4. Conclusions

A series of porous biochar products (DMC) were prepared from dried dairy manure (DM) at high pyrolysis temperatures (500–900 °C). The following conclusions were summarized:

1. According to the data on the thermogravimetric analysis (TGA) of DM, it is better to produce highly porous DMC at temperature above 500 °C because of the intense devolatilization of its lignocellulosic compositions and the increase in the aromaticity.
2. The optimal DMC product produced at 900 °C showed its BET surface area of 361 m²/g and total pore volume of 0.24 cm³/g.

3. From the N₂ adsorption–desorption isotherms with the hysteresis loops (H4 type), the DMC products are complex carbon materials, which contained both micropores (Type I) and mesopores (Type IV).
4. The carbon contents of the biochar products (i.e., DMC) significantly increased to above 50% during the carbonization process.
5. The cation exchange capacity (CEC) of the optimal DMC product showed a high value of 57.5 ± 16.1 cmol/kg.

Author Contributions: Conceptualization, W.-T.T.; methodology, P.-C.H.; validation, P.-C.H.; data curation, Y.-Q.L.; formal analysis, Y.-Q.L.; writing—original draft preparation, W.-T.T.; writing—review and editing, W.-T.T.

Funding: This research received no external funding.

Acknowledgments: The authors express sincere appreciations to the Instrument Centers of National Chung Hsing University, National Tsing-Hua University and National Pingtung University of Science & Technology for their supports in the analyses of organic elements, inorganic elements and scanning electron microscope- energy dispersive X-ray spectroscopy (SEM-EDS), respectively.

Conflicts of Interest: The authors declare no conflict of interest.

References

1. Intergovernmental Panel on Climate Change (IPCC). *2006-IPCC Guidelines for National Greenhouse Gases Inventories*; IPCC: Geneva, Switzerland, 2006.
2. Gerber, P.J.; Steinfeld, H.; Henderson, B.; Mottet, A.; Opio, C.; Dijkman, J.; Falcucci, A.; Tempio, G. *Tracking Climate Change Through Livestock—A Global Assessment of Emissions and Mitigation Opportunities*; Food and Agriculture Organization: Rome, Italy, 2013.
3. Cantrell, K.B.; Hunt, P.G.; Uchimiya, M.; Novak, J.M.; Ro, K.S. Impact of pyrolysis temperature and manure source on physicochemical characteristics of biochar. *Bioresour. Technol.* **2012**, *107*, 419–428. [[CrossRef](#)] [[PubMed](#)]
4. Cantrell, K.B.; Ducey, T.; Ro, K.S.; Hunt, P.G. Livestock waste-to-bioenergy generation opportunities. *Bioresour. Technol.* **2008**, *99*, 7941–7953. [[CrossRef](#)] [[PubMed](#)]
5. Basu, P. *Biomass Gasification, Pyrolysis and Torrefaction*, 2nd ed.; Academic Press: San Diego, CA, USA, 2013.
6. Tsai, W.T.; Chang, J.H.; Hsien, K.J.; Chang, Y.M. Production of pyrolytic liquids from industrial sewage sludges in an induction-heating reactor. *Bioresour. Technol.* **2009**, *100*, 406–412. [[CrossRef](#)] [[PubMed](#)]
7. Tsai, W.T.; Lee, M.K.; Chang, J.H.; Su, T.Y.; Chang, Y.M. Characterization of bio-oil from induction-heating pyrolysis of food-processing sewage using in an induction-heating reactor. *Bioresour. Technol.* **2009**, *100*, 2650–2654. [[CrossRef](#)] [[PubMed](#)]
8. Lee, M.K.; Tsai, W.T.; Tsai, Y.L.; Lin, S.H. Pyrolysis of napier grass in an induction-heating reactor. *J. Anal. Appl. Pyrolysis* **2010**, *88*, 110–116. [[CrossRef](#)]
9. Lehmann, J.; Joseph, S. Biochar for environmental management: An introduction. In *Biochar for Environmental Management*, 2nd ed.; Lehmann, J., Joseph, S., Eds.; Routledge: New York, NY, USA, 2015; pp. 1–13.
10. Cao, X.; Ma, L.; Gao, B.; Harris, W. Dairy-manure derived biochar effectively sorbs lead and atrazine. *Environ. Sci. Technol.* **2009**, *43*, 3285–3291. [[CrossRef](#)] [[PubMed](#)]
11. Cao, X.; Harris, W. Properties of dairy-manure-derived biochar pertinent to its potential use in remediation. *Bioresour. Technol.* **2010**, *101*, 5222–5228. [[CrossRef](#)] [[PubMed](#)]
12. Uchimiya, M.; Cantrell, K.B.; Hunt, P.G.; Novak, J.M.; Chang, S. Retention of heavy metals in a Typic Kandiodult amended with different manure-based biochars. *J. Environ. Qual.* **2012**, *41*, 1138–1149. [[CrossRef](#)]
13. Qian, L.B.; Chen, B.L. Dual role of biochars as adsorbents for aluminum: The effects of oxygen-containing organic components and the scattering of silicate particles. *Environ. Sci. Technol.* **2013**, *47*, 8759–8768.
14. Xu, X.Y.; Cao, X.D.; Zhao, L.; Wang, H.L.; Yu, H.R.; Gao, B. Removal of Cu, Zn, and Cd from aqueous solutions by the dairy manure-derived biochar. *Environ. Sci. Pollut. Res.* **2013**, *20*, 358–368. [[CrossRef](#)]

15. Zhu, Y.; Yi, B.J.; Yuan, Q.X.; Wang, M.; Yan, S.P. Removal of methylene blue from aqueous solution by cattle manure-derived low temperature biochar. *RSC Adv.* **2018**, *8*, 19917–19929. [[CrossRef](#)]
16. Chen, Z.L.; Zhang, J.Q.; Huang, L.; Yuan, Z.H.; Li, Z.J.; Liu, M.C. Removal of Cd and Pb with biochar made from dairy manure at low temperature. *J. Integr. Agric.* **2019**, *18*, 201–210. [[CrossRef](#)]
17. Zhao, B.; Xu, H.; Ma, F.; Zhang, T.; Nan, X. Effects of dairy manure biochar on adsorption of sulfate onto light sierozem and its mechanisms. *RSC Adv.* **2019**, *9*, 5218–5223. [[CrossRef](#)]
18. Jindo, K.; Sonoki, T. Comparative assessment of biochar stability using multiple indicators. *Agronomy* **2019**, *9*, 254. [[CrossRef](#)]
19. Fu, P.; Hu, S.; Xiang, J.; Sun, L.; Su, S.; Wang, J. Evaluation of the porous structure development of chars from pyrolysis of rice straw: Effects of pyrolysis temperature and heating rate. *J. Anal. Appl. Pyrolysis* **2012**, *98*, 177–183. [[CrossRef](#)]
20. Park, J.H.; Wang, J.J.; Meng, Y.L.; Wei, Z.; DeLaune, R.D.; Seo, D.C. Adsorption/desorption behavior of cationic and anionic dyes by biochars prepared at normal and high pyrolysis temperatures. *Colloids Surf. A* **2019**, *572*, 274–282. [[CrossRef](#)]
21. Liu, S.C.; Tsai, W.T. Thermochemical characteristics of dairy manure and its derived biochars from a fixed-bed pyrolysis. *Int. J. Green Energy* **2016**, *13*, 963–968. [[CrossRef](#)]
22. Tsai, W.T.; Liu, S.C. Thermochemical characterization of cattle manure relevant to its energy conversion and environmental implications. *Biomass Convers. Biorefin.* **2016**, *6*, 71–77. [[CrossRef](#)]
23. Tsai, T.W.; Hsu, C.H.; Lin, Y.Q. Highly porous and nutrients-rich biochar derived from dairy cattle manure and its potential for removal of cationic compound from water. *Agriculture* **2019**, *9*, 114. [[CrossRef](#)]
24. Steiner, C. Considerations in biochar characterization. In *Agricultural and Environmental Applications of Biochar: Advances and Barriers*; Guo, M., He, Z., Uchimiyama, S.M., Eds.; Soil Science Society of America: Madison, WI, USA, 2016; pp. 87–100.
25. Hung, C.Y.; Tsai, W.T.; Chen, J.W.; Lin, Y.Q.; Chang, Y.M. Characterization of biochar prepared from biogas digestate. *Waste Manag.* **2017**, *66*, 53–60. [[CrossRef](#)] [[PubMed](#)]
26. Tsai, W.T.; Huang, P.C. Characterization of acid-leaching cocoa pod husk (CPH) and its resulting activated carbon. *Biomass Convers. Biorefin.* **2018**, *8*, 521–528. [[CrossRef](#)]
27. Fan, L.T.; Chen, L.C.; Mehta, C.D.; Chen, Y.R. Energy and available energy contents of cattle manure and digester sludge. *Agric. Wastes* **1985**, *13*, 239–249. [[CrossRef](#)]
28. Wang, L.; Shahbazi, A.; Hanna, M.A. Characterization of corn stover, distiller grains and cattle manure for thermochemical conversion. *Biomass Bioenergy* **2011**, *35*, 171–178. [[CrossRef](#)]
29. Wu, H.; Hanna, M.A.; Jones, D.D. Thermogravimetric characterization of dairy manure as pyrolysis and combustion feedstocks. *Waste Manag. Res.* **2012**, *30*, 1066–1071. [[CrossRef](#)] [[PubMed](#)]
30. Baerthaler, G.; Zischka, M.; Haraldsson, C.; Obernberger, I. Determination of major and minor ash-forming elements in solid biofuels. *Biomass Bioenergy* **2006**, *30*, 983–997. [[CrossRef](#)]
31. Hsu, J.H.; Lo, S.L. Effect of composting on characterization of copper, manganese, and zinc from swine manure compost. *Environ. Pollut.* **2001**, *114*, 119–127. [[CrossRef](#)]
32. Smith, J.M. *Chemical Engineering Kinetics*, 3rd ed.; McGraw-Hill: New York, NY, USA, 1981.
33. Suzuki, M. *Adsorption Engineering*; Elsevier: Amsterdam, The Netherlands, 1990.
34. Lian, F.; Xing, B. Black carbon (biochar) in water/soil environments: Molecular structure, sorption, stability, and potential risk. *Environ. Sci. Technol.* **2017**, *51*, 13517–13532. [[CrossRef](#)]
35. Keiluweit, M.; Nico, P.S.; Johnson, M.G.; Kleber, M. Dynamic molecular structure of plant biomass-derived black carbon (biochar). *Environ. Sci. Technol.* **2010**, *44*, 1247–1253. [[CrossRef](#)]
36. Lowell, S.; Shields, J.E.; Thomas, M.A.; Thommes, M. *Characterization of Porous Solids and Powders: Surface Area, Pore Size and Density*; Springer: Dordrecht, The Netherlands, 2006.
37. Mukome, F.N.D.; Parikh, S.J. Chemical, physical, and surface characterization of biochar. In *Biochar: Production, Characterization, and Applications*; Ok, Y.K., Uchimiyama, S.M., Chang, S.X., Bolan, N., Eds.; CRC Press: Boca Raton, FL, USA, 2016; pp. 67–96.
38. Liang, B.; Lemann, J.; Solomon, D.; Kinyangi, J.; Grossman, J.; O'Neill, B.; Skjemstad, J.O.; Thies, J.; Luizao, F.J.; Petersen, J.; et al. Black carbon increases cation exchange capacity in soils. *Soil Sci. Soc. Am. J.* **2006**, *70*, 1719–1730. [[CrossRef](#)]

39. Huff, M.D.; Lee, J.W. Biochar-surface oxygenation with hydrogen peroxide. *J. Environ. Manag.* **2016**, *165*, 17–21. [[CrossRef](#)]
40. Huff, M.D.; Marshall, S.; Saeed, H.A.; Lee, J.W. Surface oxygenation of biochar through ozonization for dramatically enhancing cation exchange capacity. *Bioresour. Bioprocess.* **2018**, *5*, 18. [[CrossRef](#)]



© 2019 by the authors. Licensee MDPI, Basel, Switzerland. This article is an open access article distributed under the terms and conditions of the Creative Commons Attribution (CC BY) license (<http://creativecommons.org/licenses/by/4.0/>).